International Journal of
INTELLIGENT SYSTEMS AND APPLICATIONS IN ENGINEERING

ISSN:2147-6799 www.ijisae.org Original Research Paper

# Enhancing Brain Tumor Diagnosis: A Comprehensive AI Approach Using BTuNet for Classification of MRI Images

**Dr. R. Murugadoss[1*], Dr. Lekshmy P L[2], Dr. Sivaraj Rengaraj[3], Dr. Mamta Jagdish Baheti[4] Dr.G.Kavitha[5]**

**Submitted:** 25/01/2024 **Revised:** 07/03/2024 **Accepted:** 15/03/2024

**Abstract***:* A brain tumor is an abnormal growth in the brain or spinal canal, classified as benign or malignant. MRI is crucial for diagnosis, especially in distinguishing between conditions like glioma, meningioma, non-tumor cases, and pituitary conditions. Manual interpretation by radiologists, the traditional method, is time-consuming, subjective, and prone to error. AI models are essential for improving brain tumour diagnosis accuracy, consistency, objectivity, and early detection. This leads to better patient outcomes and more efficient healthcare delivery. This research aim to develop an AI based diagnosis model named BTuNet to classify the MRI brain image like glioma, meningioma, non-tumor cases, and pituitary conditions. The research employs a Gaussian filter for preprocessing and utilizes BTuNet for feature extraction and classification. The outcomes show that the proposed BTuNet achieves superior performance in classifying MRI brain images in all the measures employed, especially with an accuracy of 98%, surpassing other state-of-the-art techniques. The research contributes valuable insights, enhancing diagnostic tools and methodologies, with potential benefits for timely medical interventions and improved patient outcomes.

***Keywords****: brain tumor, MRI images, BTuNet, glioma, meningioma, non-tumor cases, and pituitary, VGG-19, Long short-term memory.*

## 1. Introduction

For an early diagnosis and treatment planning, brain tumor detection and analysis are essential. Over the years, extensive research and procedural development have been undertaken in this field [1]. Since the precision of tumor detection is crucial, a number of segmentation algorithms have been created to improve the classification accuracy of brain tumor [2, 3]. Brain image segmentation remains a complex and challenging task within the domain of medical image processing [4]. Despite advancements in brain tumor detection, there is a continued need for more effective and automated systems to improve accuracy [5]. Traditional methods of manual inspection of MRI images are time-consuming and subject to human error [6]. Automated systems, driven by advancements in image processing and machine learning [7], have emerged as promising solutions to enhance the efficiency and accuracy of brain tumor detection [8].

.

Developing an extremely effective AI-based diagnostic model for the categorization of MRI brain images is the main objective of this research [9, 10]. The focus is specifically on accurately categorizing diverse conditions including glioma, meningioma, non-tumor cases, and pituitary conditions [11, 12].

*1HoD, Artificial Intelligence and Data Science, V.S.B. College of Engineering Technical campus,Coimbatore,India.*
*Orcid id: https://orcid.org/0009-0006-4909-0678*
*2Assistant Professor in CSE, LBS Institute of Technology for Women, Thiruvananthapuram, Kerala, India.*
*Orcid id: https://orcid.org/0009-0000-4727-8788*
*3Department of pharmacology, Aarupadai Veedu Medical college & Hospital, India.*
*Orcid id: https://orcid.org/0009-0007-2976-0029*
*4Assistant Professor and HOD, Hislop college, Nagpur, Maharashtra,India*
*Orcid id: https://orcid.org/0009-0003-8469-0722*
*5Professor,Computer Science and Engineering, Muthayammal Engineering College, Rasipuram, India.*
*Orcid id: https://orcid.org/0009-0001-8143-4155*
** Corresponding Author Email: drrmdccse@gmail.com*

The methodology adopted in this research follows a multi-step process, commencing with the application of a Gaussian filter for preprocessing MRI images [13]. The research endeavors to construct an AI-based diagnostic model, termed BTuNet, which is a fusion of CNN using the VGG-19 architecture [14] and RNN [15]. This integrated model is designed for the precise classification of MRI brain images.

This research is important because it may transform brain tumor early diagnostics by providing a reliable and effective automated method. The developed system not only addresses the challenges associated with manual analysis but also contributes to the broader field of medical imaging and artificial intelligence. The outcomes of this study are expected to enhance the accuracy of brain tumor diagnosis, ultimately leading to enhanced patient outcomes and more effective treatment strategies [16].

The remaining sections of the paper are organized as follows: Section 2 provides a literature review, while Section 3 presents a detailed explanation of the proposed BTuNet. Section 4 discusses the results and their interpretation. Finally, the research concludes with a dedicated conclusion section, followed by the references.

## Literature Review

A literature review serves as a crucial step in the research process, guiding the development of new insights, methodologies, and technologies in the domain of MRI brain tumor classification. It provides a comprehensive understanding of the current state of the field and lays the groundwork for advancing research in this critical area of medical imaging. This literature review provides valuable insights into recent advancements in the classification of MRI brain images, specifically focusing on brain tumor detection.

Vankdothu et al. [17] (2022) present an automated scheme that incorporates adaptive filtering, improved K-means clustering, and deep learning utilizing Recurrent Convolutional Neural Networks (RCNN). The proposed method achieves superior outcomes in classifying gliomas, meningiomas, non-tumors, and pituitary tumors, outperforming existing methods with an accuracy of 95.17%.

For accurate brain tumor classification and segmentation, Masood et al. [18] (2021) suggest a bespoke Mask Region-based Convolution Neural Network (Mask RCNN) with a densenet-41 backbone. The model achieves 96.3% segmentation accuracy and 98.34% classification accuracy, showing improved resilience over the state-of-the-art methods.

Amin et al. [19] (2020) present an automated method for differentiating between cancerous and non-cancerous brain MRI images using Support Vector Machine classification. The proposed framework achieves an average accuracy of 97.1%, 0.98 area under the curve, 91.9% sensitivity, and 98.0% specificity, offering improved accuracy and efficiency compared to existing approaches.

Pareek et al. [20](2018) present a method utilizing supervised classification and textural feature extraction for the identification and categorization of brain tumors. The experimental results show that the Kernel Support Vector Machine (KSVM) achieves an impressive 97% accuracy, providing a reliable method for tumor classification.

Xie et al. [21] (2022) introduces the Zebra Optimization Algorithm (ZOA), inspired by the foraging and defense behavior of zebras. ZOA is assessed utilizing a variety of benchmark functions and is mathematically modeled. It outperforms nine other methods. Additionally, ZOA's effectiveness is tested on real-world engineering design problems, showcasing its capability in optimizing design variables when compared to competitors.

These studies reveal the continuous advancements in AI-based diagnostic models for MRI brain image classification, showcasing improved accuracy, efficiency, and robustness in the detection and classification of brain tumors. The insights gained from this literature review inform the development of the proposed AI-based diagnostic model in this research, contributing to the ongoing progress in the field.

## Proposed Methodology

The primary objective of this research is to create a highly efficient AI-based diagnostic model tailored for classifying MRI brain images, specifically targeting different conditions such as glioma, meningioma, non-tumor cases, and pituitary conditions. As illustrated in Fig. 1, the overall research flow for MRI brain image classification encompasses multi-step process, starting with the utilization of a Gaussian filter for preprocessing the MRI images. This preprocessing step is vital for refining and improving the quality of the

input data, reducing noise, and enhancing the overall efficacy of subsequent analyses.

Following the preprocessing phase, the research utilizes the proposed BTuNet for feature extraction and classification. BTuNet is a sophisticated model that combines elements of Convolutional Neural Network (CNN) [22, 23], specifically VGG-19 architecture, and Recurrent Neural Network (RNN), signified by the Long Short-Term Memory (LSTM) network [24]. This hybrid structure is designed to leverage the strengths of both CNN, which excels at image feature extraction, and RNN, known for its ability to capture sequential dependencies and patterns within data. The CNN component (VGG-19) [25] is adept at automatically identifying and extracting intricate visual features from the preprocessed MRI images. The LSTM network contributes to a more thorough understanding of the image data by capturing temporal dependencies and sequential information simultaneously. By combining these two neural network architectures, BTuNet aims to provide a nuanced and detailed analysis of MRI brain images, enhancing the model's capacity to accurately classify diverse brain conditions.

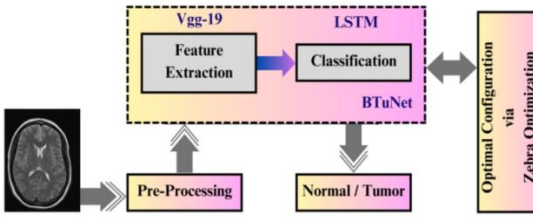


**Fig. 1.** Overall Research Flow for MRI Brain Image Classification

Dataset Description

The dataset is sourced from Kaggle's Brain Tumor MRI Dataset, designed for the classification of brain tumors. It comprises 7023 human brain MRI images categorized into four classes: glioma (1621 images), meningioma (1645 images), non-tumor (2000 images), and pituitary (1757 images). 80% of the dataset is utilized for training purposes, while the remaining 20% is utilized for testing.

**Preprocessing**

Preprocessing is mainly utilised to improve image quality, fix flaws, and get the data ready for later processes like feature extraction and classification. A Gaussian filters [26], employed in the preprocessing of MRI brain images, is a mathematical function that smoothens and reduces noise in the images. By applying a weighted averaging technique based on a bell-shaped curve, the filter helps enhance the overall quality of the images. The use of a Gaussian filter is particularly valuable in tasks such as tumor detection, aiding in the standardization of image quality and preventing overfitting in subsequent analysis or machine learning models. In this study, a Gaussian filter is employed to reduce error. Consider the input image A (i, j) which consists of some noises, to eliminate the noise present in the image, a Gaussian filter f(u, v) is applied. The mathematical expression is given in Equation (1).

$$A_G(i,j) = \sum_{u,v} A(i+u, j+v) f(u,v) \tag{1}$$

$$f(u,v) = \frac{1}{2\pi\sigma^2} \tag{2}$$

In Equation (2), u represents the horizontal distance, v represents the vertical distance and σ is the standard deviation. Fig. 2 showcases sample MRI brain images from four classes (glioma, meningioma, non-tumor cases, and pituitary) along with the corresponding pre-processed images using a Gaussian filter. Additionally, the figure includes the histogram chart for reference.

**Original image**

**Gaussian filtered image**

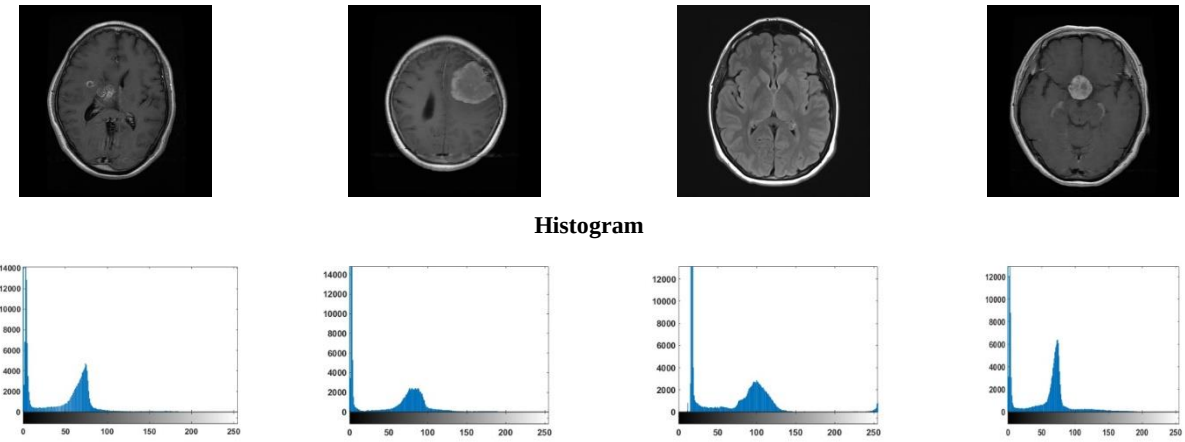


**Fig. 2.** Sample database images

**Brain Tumor Network (BTuNet)**

BTuNet, a fusion of Convolutional Neural Network (VGG-19) and LSTM, presents several advantages for brain tumor classification. By combining spatial and temporal analysis, it comprehensively extracts features from MRI images, leading to enhanced accuracy in distinguishing various tumor types. Its capacity to handle sequential data, crucial in medical imaging, allows for effective analysis of tumor progression over multiple scans. BTuNet's adaptability and specialized approach make it well-suited for medical imaging tasks, demonstrating robust classification performance and generalization across diverse datasets.

**Feature Extraction**

Feature extraction is crucial in applications where the original data is complex and contains more information than needed for a specific task. By focusing on relevant features, subsequent classification becomes more efficient and accurate. The extracted features from MRI brain images are used to train the LSTM model for tumor classification. This research incorporates VGG-19, convolutional neural network architecture renowned for its depth and uniformity, frequently employed for feature extraction and classification. The preprocessed images traverse the 19 layers, including convolutional and pooling layers, capturing hierarchical features at different scales. Subsequently, the data is compressed and introduced into fully connected layers, which acquire complex correlations between the attributes that are extracted. The intermediate layers, particularly those preceding the fully connected layers, serve as potent feature extractors, capturing low to high-level features. Effective feature extraction is made possible by the utilization of VGG-19, which makes it possible to apply that approach to the study of medical images for tasks such as tumor diagnosis and classification in MRI scans.

There are 19 layers in the VGG-19 convolutional neural network, comprising 3 fully connected layers and 16 convolution layers. Because each convolutional layer has 33 filters, this frequently utilized image classification approach was trained on the ImageNet database. The model utilizes 16 layers for feature extraction and the subsequent 3 layers for classification. Utilizing five feature extraction layer sets and max-pooling layers, it receives an input image of size 224 by 224 pixels and outputs the label. Feature extraction involves the use of a pre-trained VGG-19 model, while other machine learning techniques handle classification. To reduce the size of the feature vector computed by the CNN model post feature extraction, Locality Preserving Projection achieves dimensionality reduction, followed by a classification technique.

**Long short-term memory (LSTM)**

A two-step approach combining CNN and LSTM networks is the suggested method for classifying brain tumors. Initially, the VGG-19 model, a pre-trained deep neural network, is employed to extract discriminative features from MRI brain images. These features, which capture intricate patterns within the images, are then organized into sequences to account

for the sequential nature of volumetric MRI data. Subsequently, an LSTM model is designed to receive these feature sequences as input and learn temporal dependencies, enabling it to effectively classify brain tumors. During training, the model undergoes optimization on a dataset, with a focus on performance metrics. Further fine-tuning and optimization steps are undertaken to enhance the model's robustness. Once validated, the model can be deployed for real-world usage, with careful consideration of ethical guidelines and compliance with medical regulations to ensure its safe and responsible application in clinical settings. The LSTM is like a smart system that helps in understanding and remembering information in sequences, such as MRI brain images. It has gates like input, forget, and output gates that control the flow of information. These gates prevent problems that earlier systems had, like forgetting important details or having trouble with long-term information. The LSTM uses memory storage cells and gate mechanisms to tackle these issues. Each gate has a mathematical equation that guides how it works to manage and remember data over time.

The forget gate $F^t$ helps the LSTM determine what data needs to be provided and deleted through the cell state based on the preceding hidden structure defined by Equation (3).

$$F^t = \sigma\left(W_f \cdot \left[H^{t-1}, X^t\right] + B_f\right) \quad (3)$$

Where Ht− 1 represent the previous gate, Xt represent the input data, σ(.) represent the sigmoid activation function, Wf represent the weight measurements, and Bf represent the bias vector.

Which data will be transferred to the subsequent candidate's cell state C̃t is determined by Equation (4) and the input gate It is determined by Equation (5).

$$\tilde{C}^t = \tanh\left(W_{c.}\left[H^{t-1}, X^t\right] + B_c\right) \quad (4)$$

$$I^t = \sigma\left(W_i \cdot \left[H^{t-1}, X^t\right] + B_i\right) \quad (5)$$

Where tanh (.) denotes the hyperbolic tangent function.

The updated new cell state Ct is created by Equation (6) relating the old cell state Ct− 1 and the new candidate's cell state C̃t.

$$C^t = F^t * C^{t-1} + I^t * \tilde{C}^t \quad (6)$$

The output gate Ot denoted by Equation (7) is then created to control the LSTM cell's outcome. The desired result Ht is indicated by Equation (8) the following, which is the combination of Ot and the cell state Ct activated by the tanh function.

$$O^t = \sigma\left(W_o \cdot \left[H^{t-1}, X^t\right] + B_o\right) \quad (7)$$

$$H^t = O^t \cdot \tanh\left(C^t\right) \quad (8)$$

In order to manage long-term dependencies in information and swiftly extract sequential characteristics utilising period, we made use of the LSTM classifier's exceptional high-performance capacity.

LSTM for MRI brain image classification, optimal weight parameters are crucial for effective learning. These weights impact feature extraction, adaptability to task complexity, handling of long-term dependencies, prevention of overfitting or underfitting, improved generalization, and efficient training convergence. Manually or trial-and-error finding of optimal weights is intricate, time-consuming, and biased, especially with large datasets and complex architectures. To address these challenges, researchers integrate optimization techniques, providing a systematic and automated approach for efficient weight search, enhancing performance, reducing subjectivity, and ensuring adaptability to changes.

**Zebra Optimization Algorithm (ZOA)**

The ZOA distinguishes itself in the quest for identifying optimal weights for LSTM networks by leveraging inspiration from zebras' intelligent behaviors. Emulating the foraging and defense strategies observed in nature, ZOA exhibits diversity and adaptability, proving effective in exploring the complex and nonlinear weight solution space. Its unique biological foundation positions it as a potential solution for optimizing LSTM weights, with versatility across domains. The Fig. 3 exhibits the Flow chart of zebra optimization algorithm.

**Initial solution**

Each zebra's location in the search space is correlated with the values of the decision variables. As an outcome, a vector can be utilized to represent a zebra inside the ZOA, where the elements stand for the values of the issue variables. The entire population of zebras can be aptly modeled utilizing a matrix. Interestingly, in the first stage, zebra places in the search space are assigned at random, which starts the process of looking for possible answers.

The ZOA population matrix is specified Equation in (9).

$$X = \begin{bmatrix} X_1 \\ \vdots \\ X_i \\ \vdots \\ X_N \end{bmatrix}_{N\times m} = \begin{bmatrix} x_{1,1} & \cdots & x_{1,j} & \cdots & x_{1,m} \\ \vdots & \ddots & \vdots & \iddots & \vdots \\ x_{i,1} & \cdots & x_{i,j} & \cdots & x_{i,m} \\ \vdots & \iddots & \vdots & \ddots & \vdots \\ x_{N,1} & \cdots & x_{N,j} & \cdots & x_{N.m} \end{bmatrix}_{N\times m} \quad (9)$$

Where X is the zebra population, Xi is the ith zebra, xi,j is the value for the jth problem variable proposed by the ith zebra, N is the number of population members (zebras), and m is the number of decision variables.

Every zebra symbolizes a candidate solution to the optimization problem. This implies that the proposed values assigned to each zebra for the problem variables can be utilized to evaluate the objective function. The resulting objective function values are then compiled into a vector, as outlined in Equation (10). This vector encapsulates the outcomes of the objective function across the zebras, providing a comprehensive overview of the optimization landscape based on the initial solutions generated by the zebras in the search space.

$$F = \begin{bmatrix} F_1 \\ \vdots \\ F_i \\ \vdots \\ F_N \end{bmatrix}_{N\times 1} = \begin{bmatrix} F(X_1) \\ \vdots \\ F(X_i) \\ \vdots \\ F(X_N) \end{bmatrix}_{N\times 1}$$

(10)

Where Fi is the objective function value obtained for the ith zebra and F is the vector of objective function values. By comparing the values acquired for the objective function, it is possible to determine which candidate solution is optimal for the given problem and to analyses the quality of the related candidate solutions. The zebra with the lowest objective function value is the best possible candidate solution in minimization issues. On the other hand, the optimal candidate solution in a maximization problem is the zebra with the highest value of the objective function. Every iteration involves updating the values of the objective function due to changes in the zebra positions; hence it is also necessary to determine the best candidate solution each time.

ZOA members have been updated utilizing two of the zebra's natural behaviours. These two categories of conduct consist of

Foraging and

Defense strategies against predators.

Consequently, within each iteration, the ZOA update its population members through two distinct phases.

Foraging Behavior

In the initial phase, ZOA simulates zebra foraging behavior to update its population. The best-performing member becomes the pioneer zebra, akin to plains zebras, influencing others in the search space. This process mirrors how zebras adapt their diet based on vegetation availability, with the pioneer grazer creating conditions for other species. The foraging phase involves updating zebra positions mathematically, guided by the pioneer zebra's location (Equations 11 and 12).

$$x_{i,j}^{new,P1} = x_{i,j} + r \cdot \left(PZ_j - I \cdot x_{i,j}\right) \quad (11)$$

$$X_i = \begin{cases} X_i^{new,P1} & F_i^{new,P1} < F_i; \\ X_i & else \end{cases} \quad (12)$$

Where $X_i^{new,P1}$ is the new status of the ith zebra based on first phase, $X_{i,j}^{new,P1}$ is its jth dimension value, $F_i^{new,P1}$ is its objective function value, PZ is the pioneer zebra which is the best member, PZj is its jth dimension, r is a random number in interval [0, 1], I round (1 rand), where rand is a random number in the interval [0, 1]. Thus, $I\epsilon\{1,2\}$ and if parameter I=2, then there are much more changes in population movement.

Defense Strategies against Predators

In the subsequent phase, ZOA updates its population positions by simulating zebras' defense strategy against predators. Zebras employ different tactics based on the predator type – escaping in a zigzag pattern against lions and adopting an aggressive approach by gathering against smaller predators like hyenas. During this

defense phase, the ZOA design assumes one of two conditions with equal probability.

The lion attacks the zebra, and thus, the zebra chooses an escape strategy;

Other predators attack the zebra, and the zebra will choose the offensive strategy.

In the first strategy, when the zebras are attacked by lions, the zebras escape from the lion's attack in the vicinity of the situation in which they are located. Therefore, mathematically, this strategy can be modeled using the mode S1. In the second strategy, when other predators attack one of the zebras, the other zebras in the herd move towards the attacked zebra and try to frighten and confuse the predator by creating a defensive structure. This strategy of zebras is mathematically modeled using the mode S2 in (13). In updating the position of zebras, the new position is accepted for a zebra if it has a better value for the objective function in that new position. This update condition is modeled using Equation (13) and Equation (14).

$$X_{i,j}^{new,P2}=\begin{cases} S_1: x_{i,j}+R\cdot(2r-1)\cdot\left(1-\dfrac{t}{T}\right)\cdot x_{i,j}, & P_s\le 0.5; \\ S_2: x_{i,j}+r\cdot\left(AZ_j-I\cdot x_{i,j}\right), & else \end{cases} \quad (13)$$

$$X_i=\begin{cases} X_i^{new,P2}, & F_i^{new,P2}<F_i; \\ X_i, & else, \end{cases} \quad (14)$$

Where $X_i^{new,P2}$ is the new status of the ith zebra based on first phase, $X_{i,j}^{new,P2}$ is its jth dimension value, $F_i^{new,P2}$ is its objective function value, t is the iteration contour, T is the maximum number of iterations, R is the constant number equal to 0.01, Ps is the probability of choosing one of two strategies that are randomly generated in the interval [0, 1], AZ is the status of attacked zebra, and AZj is its jth dimension value.

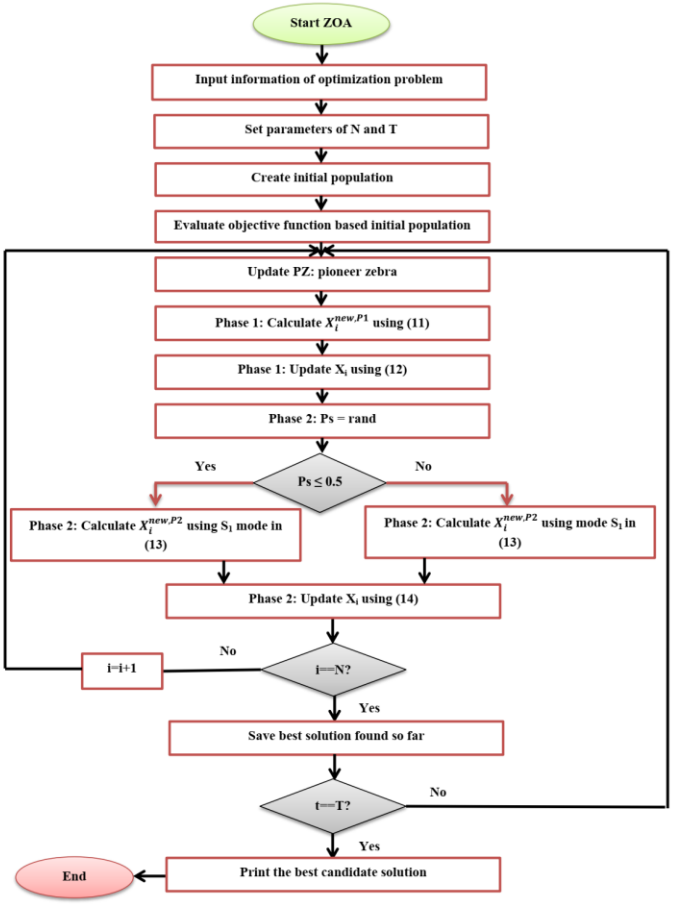


**Fig. 3.** Flow chart of Zebra Optimization Algorithm

**Results and Discussion**

The performance of the developed BTuNet model is assessed using a comprehensive set of standard measures, including Accuracy, False Discovery Rate (FDR), False Negative Rate (FNR), False Positive Rate (FPR), Matthews's correlation coefficient (MCC), Negative Predictive Value (NPV), Positive Predictive Value (PPV), Sensitivity, and Specificity. These analyses provide a thorough understanding of the proposed approach's performance, offering insights into its strengths and advantages compared to state-of-the-art methods in the domain of brain tumor classification in MRI images. Table 2 illustrates Mathematical Expression of Performance Evaluation Metrics for Proposed Predictive Models.

**Table 1.** Mathematical Expression of Performance Evaluation Metrics for Proposed Predictive Models

| Evaluation Metrics | Mathematical Expression | BTuNet (ZOA) |
|---|---|---|
| **Accuracy** | $\frac{Number\ of\ True\ Positives + Number\ of\ True\ Negatives}{Number\ of\ True\ Positives + Number\ of\ True\ Negatives + Number\ of\ False\ Positives + Number\ of\ False\ Negatives}$ | 98% |
| **FDR** | $\frac{Number\ of\ False\ Positives}{Number\ of\ False\ Positives + Number\ of\ True\ Positives}$ | 2.66% |
| **FNR** | $\frac{Number\ of\ False\ Negatives}{Number\ of\ False\ Negatives + Number\ of\ True\ Positives}$ | 1.35% |
| **FPR** | $\frac{Number\ of\ False\ Positives}{Number\ of\ False\ Positives + Number\ of\ True\ Negatives}$ | 2.63% |
| **MCC** | $\frac{TP*TN - FP*FN}{\sqrt{(TP+FP)(TP+FN)(TN+FP)(TN+FN)}}$ | 96% |
| **NPV** | $\frac{Number\ of\ True\ Negatives}{Number\ of\ True\ Negatives + Number\ of\ False\ Negatives}$ | 98.66% |
| **PPV** | $\frac{Number\ of\ True\ Positives}{Number\ of\ True\ Positives + Number\ of\ False\ Positives}$ | 97.33% |
| **Sensitivity** | $\frac{Number\ of\ True\ positives}{Number\ of\ True\ positives + Number\ of\ False\ Negatives}$ | 98.64% |
| **Specificity** | $\frac{Number\ of\ True\ Negatives}{Number\ of\ True\ Negatives + Number\ of\ False\ Positives}$ | 97.36% |

The following Fig. 4 to fig. 12 exhibits the detailed evaluation results for various techniques employed in the classification of MRI brain images, including traditional models like Lenet [27], CNN+SVM [28], DenseNet 201 [29], GAN [30], DCGAN [31], and VGG-19 [32], as well as the proposed BTuNet model and its variants incorporating Particle Swarm Optimization (PSO) and ZOA. Several key performance metrics are considered, providing a comprehensive view of each technique's classification efficacy.

Starting with Accuracy, a holistic measure of overall correctness is impressively high for BTuNet with ZOA at 0.98, highlighting its excellence in achieving correct classifications across all categories. This is particularly significant in medical diagnostics where accuracy is pivotal for reliable results. The FDR, FNR and FPR collectively provide insights into the misclassifications. BTuNet with ZOA exhibits low FDR (0.0267), FNR (0.0135) and FPR (0.0263) signifying a minimal

occurrence of false positives, false negatives, and overall misclassifications. MCC a comprehensive metric considering all elements of the confusion matrix, is impressively high at 0.9601 for BTuNet with ZOA. This suggests a robust balance between sensitivity and specificity, reflecting the model's overall performance.

NPV representing the precision of negative predictions is commendably high for BTuNet with ZOA at 0.9867. This emphasizes the model's capability to accurately predict negative instances, reducing false negatives. Precision, indicated by PPV showcases the precision of positive predictions. BTuNet with ZOA demonstrates high precision at 0.9733, underlining its reliability in correctly classifying positive instances, minimizing false positives.

Sensitivity, the BTuNet integrated with ZOA achieves the highest score (0.9865), demonstrating its effectiveness in correctly identifying positive instances such as glioma, meningioma, non-tumor cases, and pituitary conditions. This heightened sensitivity is particularly crucial in medical imaging applications where accurately detecting true positive cases is essential. Additionally, the specificity of BTuNet with ZOA is notable, reaching 0.9737. This value highlights the model's ability to accurately identify negative instances, indicating effective discrimination between cases with and without the conditions of interest.

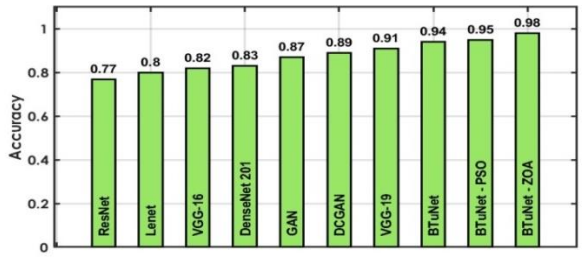


**Fig. 4.** Accuracy as a Performance Evaluation Metric for MRI Brain Image Classification

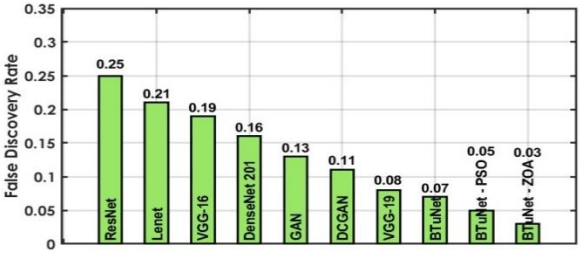


**Fig. 5.** FDR as a Performance Evaluation Metric for MRI Brain Image Classification

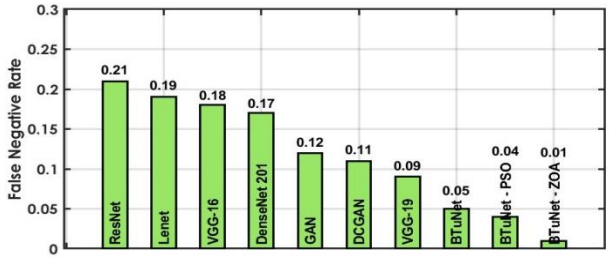


**Fig. 6.** FNR as a Performance Evaluation Metric for MRI Brain Image Classification

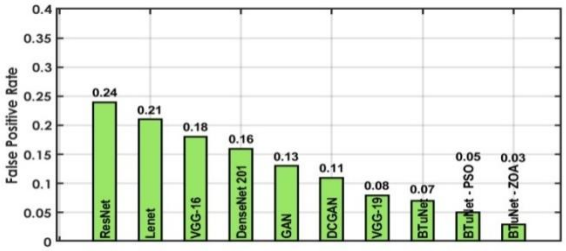


**Fig. 7.** FPR as a Performance Evaluation Metric for MRI Brain Image Classification

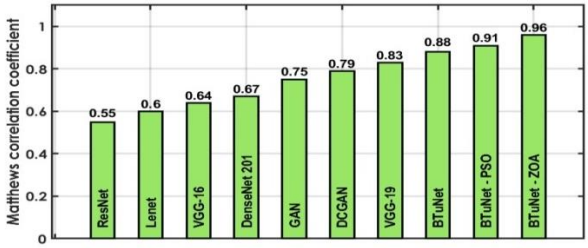


**Fig. 8.** MCC as a Performance Evaluation Metric for MRI Brain Image Classification

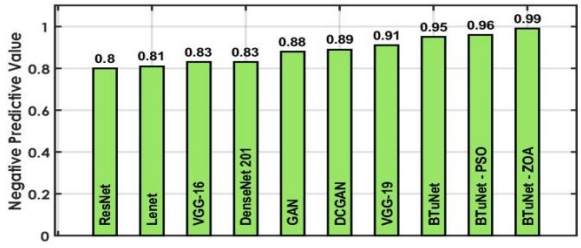


**Fig. 9.** NPV as a Performance Evaluation Metric for MRI Brain Image Classification

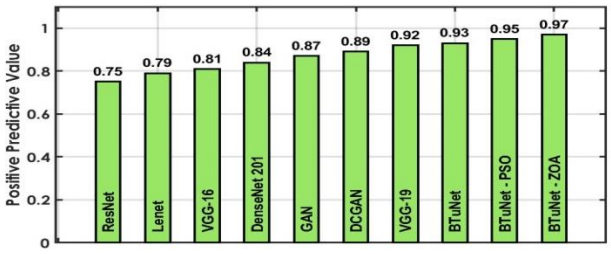


**Fig. 10.** PPV as a Performance Evaluation Metric for MRI Brain Image Classification

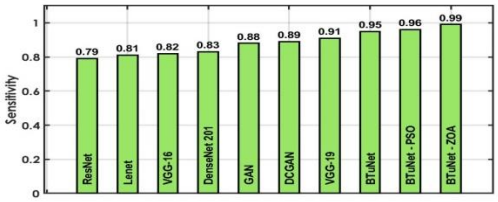


**Fig. 11.** Sensitivity as a Performance Evaluation Metric for MRI Brain Image Classification

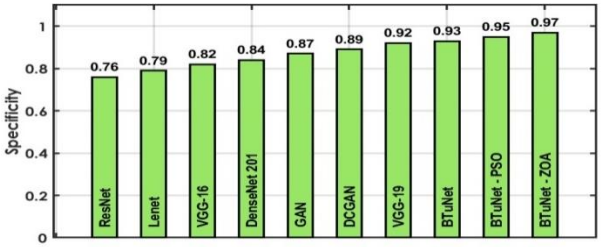


**Fig. 12.** Specificity as a Performance Evaluation Metric for MRI Brain Image Classification

Eventually, BTuNet with ZOA consistently outperforms other techniques across a spectrum of metrics, indicating its superiority in accurately classifying MRI brain images. The integration of ZOA evidently enhances the model's ability to identify optimal weights for the LSTM, resulting in a highly effective and reliable classification tool for brain tumor detection in medical imaging.

## Conclusion

This research introduces BTuNet, a hybrid model combining VGG-19 for feature extraction and LSTM for classification. To further enhance performance, the study integrates ZOA techniques to identify optimal weights for the LSTM model. The proposed BTuNet exhibits superior results across all evaluated measures, notably achieving a maximum accuracy of 98%. This integrated approach demonstrates the efficacy of leveraging both deep learning architectures and nature-inspired optimization techniques for brain tumor classification in MRI images. For future work, exploring the scalability and adaptability of the BTuNet model to diverse datasets and potentially incorporating advancements in deep learning or optimization algorithms could be promising avenues for research.


## Declaration of Conflicting Interests

The authors declared no potential conflicts of interest with respect to the research, authorship, and/or publication of this article.

## Funding

The authors received no financial support for the research, authorship, and/or publication of this article.


## References


[1] H. Dong, G. Yang, F. Liu, Y. Mo, and Y. Guo, "Automatic brain tumor detection and segmentation using U-Net based fully convolutional networks," In Medical Image Understanding and Analysis: 21st Annual Conference, MIUA 2017, Edinburgh, UK, July 11–13, 2017, Proceedings 21, pp. 506-517. Springer International Publishing, 2017. https://doi.org/10.1007/978-3-319-60964-5_44

[2] N. Kumari, and S. Saxena, "Review of brain tumor segmentation and classification," In 2018 International conference on current trends towards converging technologies (ICCTCT), pp. 1-6. IEEE, Mar. 2018. DOI: 10.1109/ICCTCT.2018.8551004

[3] S. R. Ashokkumar, S. Anupallavi, M. Premkumar, and V. Jeevanantha, "Implementation of deep neural networks for classifying electroencephalogram signal using fractional S-transform for epileptic seizure detection," Int. J. Imag. Syst. Tech., vol. 31, no. 2, pp.895-908, Jun. 2021. https://doi.org/10.1002/ima.22565

[4] R. Wang, T. Lei, R. Cui, B. Zhang, H. Meng, and A. K. Nandi, "Medical image segmentation using deep learning: A survey," IET Image Process., vol.16, no. 5, pp. 1243-1267, Apr. 2022. https://doi.org/10.1049/ipr2.12419

[5] E.S.A. El-Dahshan, H. M. Mohsen, K. Revett, and A.B.M. Salem, "Computer-aided diagnosis of human brain tumor through MRI: A survey and a new algorithm," Expert syst. Appl., vol.41, no. 11, pp. 5526-5545, Sep. 2014. https://doi.org/10.1016/j.eswa.2014.01.021

[6] R. A.Pizarro, X. Cheng, A. Barnett, H. Lemaitre, B. A. Verchinski, A. L. Goldman, E. Xiao, "Automated quality assessment of structural magnetic resonance brain images based on a supervised machine learning algorithm," Front. Neuroinform., vol.10, pp. 52, Dec. .2016. https://doi.org/10.3389/fninf.2016.00052

[7] A. Shoeibi, M. Khodatars, M. Jafari, P. Moridian, M. Rezaei, R. Alizadehsani, F. Khozeimeh, "Applications of deep learning techniques for automated multiple sclerosis detection using magnetic resonance imaging: A review," Comput. Biol. Med., vol.136, Sep. 2021. 104697.https://doi.org/10.1016/j.compbiomed.2021.104697

[8] K. Budati, and R.B. Katta, "An automated brain tumor detection and classification from MRI images using machine learning technique s with IoT," Environ. Dev. Sustain., vol.24, no. 9, pp. 10570-10584, Sep. 2022. https://doi.org/10.1007/s10668-021-01861-8

[9] Rehman, S. Naz, M. I. Razzak, F. Akram, and M. Imran, "A deep learning-based framework for automatic brain tumors classification using transfer learning," Circuits, Syst. Signal Process., vol. 39, pp. 757-775, Feb. 2020. https://doi.org/10.1007/s00034-019-01246-3

[10] Z. Jia, and D. Chen, "Brain Tumor Identification and Classification of MRI images using deep learning techniques," IEEE Access, Aug. 2020. DOI: 10.1109/ACCESS.2020.3016319

[11] A. B. Abdusalomov, M. Mukhiddinov, and T. K. Whangbo, "Brain tumor detection based on deep learning approaches and magnetic resonance imaging," Cancers, vol.15, no. 16, pp. 4172, Aug. 2023. https://doi.org/10.3390/cancers15164172

[12] M. F. Ahamed, M. M. Hossain, M. Nahiduzzaman, M. R. Islam, M. R. Islam, M. Ahsan, and J. Haider, "A review on brain tumor segmentation based on deep learning methods with federated learning techniques," Comput. Med. Imaging Graph., pp. 102313, Nov. 2023. https://doi.org/10.1016/j.compmedimag.2023.102313

[13] J. Shedbalkar, K. Prabhushetty, and A. Inchalc, "A comparative analysis of filters for noise reduction and smoothening of brain MRI images," In 2021 6th International Conference for Convergence in Technology (I2CT), Apr. pp. 1-6. IEEE, 2021. DOI: 10.1109/I2CT51068.2021.9417979

[14] M. Mateen, J. Wen, Nasrullah, S. Song, and Z. Huang, "Fundus image classification using VGG-19 architecture with PCA and SVD," Symmetry, vol.11, no. 1, pp.1, Dec. 2018. https://doi.org/10.3390/sym11010001

[15] A. Sherstinsky, "Fundamentals of recurrent neural network (RNN) and long short-term memory (LSTM) network," Phys. D: Nonlinear Phenom., vol.404, pp. 132306, Mar. 2020. https://doi.org/10.1016/j.physd.2019.132306

[16] S. Shahpar, P. V. Mhatre, and M. E. Huang, "Update on brain tumors: new developments in neuro-oncologic diagnosis and treatment, and impact on rehabilitation strategies," PM&R, vol.8, no. 7, pp. 678-689, Jul. 2016. https://doi.org/10.1016/j.pmrj.2015.10.012

[17] R. Vankdothu, and M. A. Hameed, "Brain tumor MRI images identification and classification based on the recurrent convolutional neural network," Meas: Sens., vol.24, pp. 100412, Dec. 2022. https://doi.org/10.1016/j.measen.2022.100412

[18] M. Masood, T. Nazir, M. Nawaz, A. Mehmood, J. Rashid, H. Y. Kwon, T. Mahmood, and A. Hussain, "A novel deep learning method for recognition and classification of brain tumors from MRI images." Diagnostics, vol.11, no. 5, Apr. 2021. 744.https://doi.org/10.3390/diagnostics11050744

[19] Amin, J. M. Sharif, M. Yasmin, and S. L. Fernandes, "A distinctive approach in brain tumor detection and classification using MRI," Pattern Recognit. Lett., vol.139, pp. 118-127, Nov. 2020, https://doi.org/10.1016/j.patrec.2017.10.036

[20] M. Pareek, C. K. Jha, and S. Mukherjee, "Brain tumor classification from MRI images and calculation of tumor area," In Soft Computing: Theories and Applications: Proceedings of SoCTA 2018, pp. 73-83. Singapore: Springer Singapore, Feb. 2020. https://doi.org/10.1007/978-981-15-0751-9_7

[21] E. Trojovská, M. Dehghani, and P. Trojovský, "Zebra optimization algorithm: A new bio-inspired optimization algorithm for solving optimization algorithm," IEEE Access, vol.10, pp.49445-49473, May. 2022. DOI: 10.1109/ACCESS.2022.3172789

[22] A. G. Devi, A. Thota, G. Nithya, S. Majji, A. Gopatoti, and L. Dhavamani, "Advancement of Digital Image Steganography using Deep Convolutional Neural Networks," In 2022 International Interdisciplinary Humanitarian Conference for Sustainability (IIHC), pp. 250-254. IEEE, Nov. 2022. DOI: 10.1109/IIHC55949.2022.10060230

[23] G. Mercy Bai, and P. Venkadesh, "Optimized Deep Neuro-Fuzzy Network with MapPeduce Architecture for Acute Lymphoblastic Leukemia Classification and Severity Analysis." Int. J. Image Graph., pp. 2450028, Feb. 2023. DOI: 10.1142/S0219467824500281

[24] X.H. Le, H. V. Ho, G. Lee, and S. Jung, "Application of long short-term memory (LSTM) neural network for flood forecasting," Water, vol.11, no. 7, pp. 1387, Jul. 2019. https://doi.org/10.3390/w11071387

[25] L. Wen, X. Li, X. Li, and L. Gao, "A new transfer learning based on VGG-19 network for fault diagnosis," In 2019 IEEE 23rd international conference on computer supported cooperative work in design (CSCWD), pp. 205-209. IEEE, May. 2019. DOI: 10.1109/CSCWD.2019.8791884

[26] H. H. Afshari, S. A. Gadsden, and S. Habibi, "Gaussian filters for parameter and state estimation: A general review of theory and recent trends," Signal Process., vol.135, pp. 218-238, Jun. 2017. https://doi.org/10.1016/j.sigpro.2017.01.001

[27] H. M. Rai, K. Chatterjee, A. Gupta, and A. Dubey, "A novel deep cnn model for classification of brain tumor from mr images," In 2020 IEEE 1st international conference for convergence in engineering (ICCE), pp. 134-138. IEEE, Sep. 2020. doi:10.1109/icce50343.2020.9290740

[28] Z. A. Sejuti, and M. S. Islam, "An efficient method to classify brain tumor using CNN and SVM," In 2021 2nd International Conference on Robotics, Electrical and Signal Processing Techniques (ICREST), pp. 644-648. IEEE, Jan. 2021. DOI: 10.1109/ICREST51555.2021.9331060

[29] S. Sharma, S. Gupta, D. Gupta, A. Juneja, H. Khatter, S. Malik, and Z. K. Bitsue, "Deep Learning Model for Automatic Classification and Prediction of Brain Tumor," J. Sens. 2022., Apr. 2022. https://doi.org/10.1155/2022/3065656

[30] N. Ghassemi, A. Shoeibi, and M. Rouhani, "Deep neural network with generative adversarial networks pre-training for brain tumor classification based on MR images," Biomed. Signal Process. Control., vol.57, pp. 101678, Mar. 2020. doi:10.1016/j.bspc.2019.101678

[31] M. Alshayeji, J. A. Buloushi, A. Ashkanani, and S.E. Abed, "Enhanced brain tumor classification using optimized multi-layered convolutional neural network architecture." Multi. Tools Appl., vol.80, no. 19, pp. 28897-28917, Aug. 2021. https://doi.org/10.1007/s11042-021-10927-8

[32] Z. N. K. Swati, Q. Zhao, M. Kabir, F. Ali, Z. Ali, S. Ahmed, and J. Lu, "Brain tumor classification for MR images using transfer learning and fine-tuning," Comput. Med. Imaging Graph., vol.75, pp. 34-46, Jul. 2019. https://doi.org/10.1016/j.compmedimag.2019.05.001